AD-A086 264 PENNSYLVANIA UNIV PHILADELPHIA DEPT OF CHEMISTRY F/G 20/12
SYNTHESIS AND PROPERTIES OF SEMICONDUCTING AND METALLIC DERIVAT--ETC(U)
SEP 78 A G MACDIARMID, A J HEEGER N00014-75-C-0962
UNCLASSIFIED TR-78-8 NL

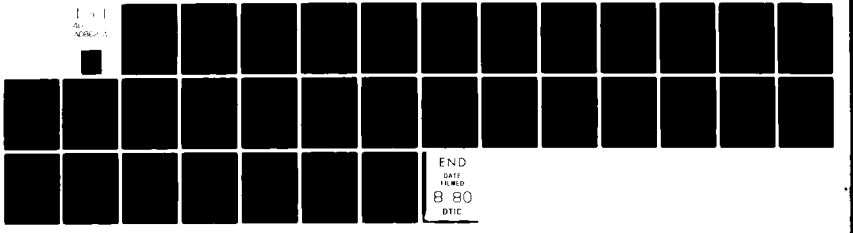

END
DATE FILMED
8 80
DTIC

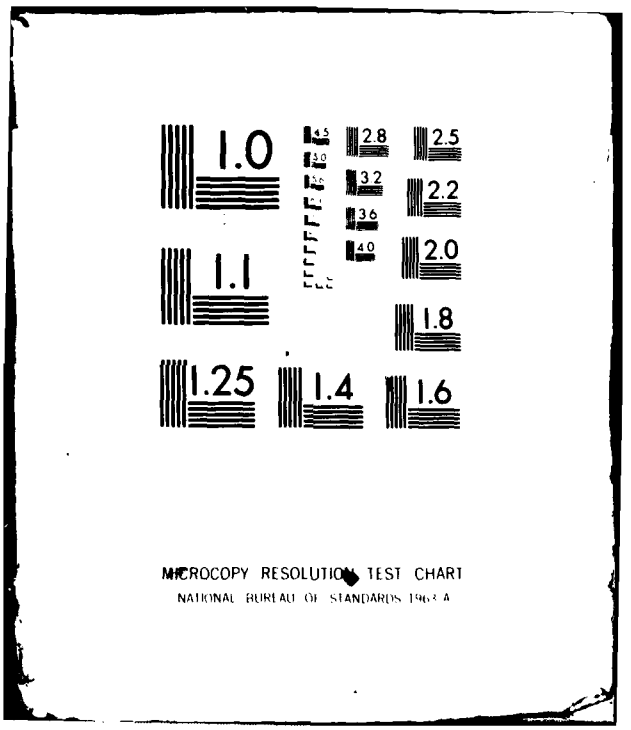
1.0
1.1
1.25
1.4
1.6
1.8
2.0
2.2
2.5
2.8
3.2
3.6
4.0
MICROCOPY RESOLUTION TEST CHART
NATIONAL BUREAU OF STANDARDS 1963-A

Unclassified

SECURITY CLASSIFICATION OF THIS PAGE (When Data Entered)

REPORT DOCUMENTATION PAGE

READ INSTRUCTIONS BEFORE COMPLETING FORM

1. REPORT NUMBER: Technical Report No. 78-8
2. GOVT ACCESSION NO.: AD-A086264
3. RECIPIENT'S CATALOG NUMBER:

4. TITLE (and Subtitle): Synthesis and Properties of Semiconducting and Metallic Derivatives of Polyacetylene, $(CH)_x$
5. TYPE OF REPORT & PERIOD COVERED: Interim Technical Report
6. PERFORMING ORG. REPORT NUMBER:

7. AUTHOR(s): Alan G. MacDiarmid and Alan J. Heeger*
8. CONTRACT OR GRANT NUMBER(s): N00014-75-C-0962

9. PERFORMING ORGANIZATION NAME AND ADDRESS: Department of Chemistry and Department of Physics*, University of Pennsylvania, Philadelphia, Pa. 19104
10. PROGRAM ELEMENT, PROJECT, TASK AREA & WORK UNIT NUMBERS: NR-356-602

11. CONTROLLING OFFICE NAME AND ADDRESS: Department of the Navy, Office of Naval Research, Arlington, Virginia 22217
12. REPORT DATE: Sept[illegible]78
13. NUMBER OF PAGES: 29

14. MONITORING AGENCY NAME & ADDRESS (if different from Controlling Office)
15. SECURITY CLASS. (of this report): Unclassified
15a. DECLASSIFICATION/DOWNGRADING SCHEDULE

LEVEL II

16. DISTRIBUTION STATEMENT (of this Report)

Distribution unlimited; approved for public release.

DTIC ELECTE JUL 7 1980 D

17. DISTRIBUTION STATEMENT (of the abstract entered in Block 20, if different from Report)

TR-78-8

18. SUPPLEMENTARY NOTES

Prepared for publication in Molecular Metals, Ed., W. E. Hatfield, NATO Conference Series, Plenum Press, New York, 1979, p. 161.

19. KEY WORDS (Continue on reverse side if necessary and identify by block number)

Semiconducting and metallic derivatives of polyacetylene, $(CH)_x$; organic polymer; electrical conductivity; insulator; semiconductor; metal; donors; acceptors; polycrystalline films; n-type or p-type semiconductors; cis-trans content; Ziegler catalyst; cis-$(CH)_x$; trans-$(CH)_x$; infrared absorption bands; solid state ^{13}C nmr studies; trans-$(CHI_{0.22})_x$; trans-$(CHBr_{0.22})_x$; cis-$[CH(AsF_5)_{0.09}]_x$; (OVER)

20. ABSTRACT (Continue on reverse side if necessary and identify by block number)

Polyacetylene, $(CH)_x$ is the simplest organic polymer. Through chemical doping, the electrical conductivity of films of $(CH)_x$ can be varied over twelve orders of magnitude with properties ranging from insulator ($\sigma<10^{-10}$ ohm^{-1}cm^{-1}) to semiconductor to metal ($\sigma>10^{3}$ ohm^{-1}cm^{-1}). Both donors and acceptors can be used with these flexible, free-standing polycrystalline polymer films (thickness 10^{-5} cm to 0.5 cm) to yield n-type or p-type material. In this review, we summarize some of the more important chemical and physical properties of $(CH)_x$ and its doped derivatives.

DD FORM 1 JAN 73 1473 EDITION OF 1 NOV 65 IS OBSOLETE S/N 0102-014-6601

Unclassified

SECURITY CLASSIFICATION OF THIS PAGE (When Data Entered)

278975

AD A086264

DDC FILE COPY

19. metallic levels; bandwidth; polymer chains; π-electrons; trans-$[Na_{0.28}(CH)]_x$; doped $(CH)_x$ films; semiconductor-metal transition; cis-$[CH(AsF_5)_{0.14}]_x$; transport studies; energy gap; far ir transmission; absorption coefficient, α; dielectric constant; magnetic studies; electron-hole pairs; photoconductivity; photo-conductive edge; oriented films; anisotropic electrical properties; temperature dependence of conductivities; Montgomery measurements; $\sigma_{//}$; $\sigma_{\perp}$; scanning electron microscope picture; anisotropic optical properties; $R_{//}$; $R_{\perp}$; p-n junction; Na-doped films; sodium naphthalide, $Na^+(C_{10}H_8)^-$; $(CHNa_{0.27})_x$; $(CHNa_{0.27}I_{0.28})_x$; thermoelectric power measurements; Schottky barrier; X-ray diffraction activation energies; mobility; Hall effect measurements.

OFFICE OF NAVAL RESEARCH

Contract N00014-75-C-0962

Task No. 356-602

TECHNICAL REPORT NO. 78-8

Synthesis and Properties of Semiconducting and Metallic Derivatives of Polyacetylene, $(CH)_x$

by

Alan G. MacDiarmid and Alan J. Heeger*

Department of Chemistry and

Department of Physics*,

University of Pennsylvania

Philadelphia, Pennsylvania 19104

September 25, 978

SYNTHESIS AND PROPERTIES OF SEMICONDUCTING AND METALLIC DERIVATIVES OF POLYACETYLENE, $(CH)_x$.

Alan G. MacDiarmid and Alan J. Heeger*

Department of Chemistry and Department of Physics,* University of Pennsylvania Philadelphia, PA 19104, U.S.A.

ABSTRACT

Polyacetylene, $(CH)_x$ is the simplest organic polymer. Through chemical doping, the electrical conductivity of films of $(CH)_x$ can be varied over twelve orders of magnitude with properties ranging from insulator ($\sigma < 10^{-10}$ ohm^{-1}cm^{-1})to semiconductor to metal ($\sigma > 10^{3}$ ohm^{-1}cm^{-1}). Both donors and acceptors can be used with these flexible, free-standing polycrystalline polymer films (thickness 10^{-5}cm to 0.5 cm) to yield n-type or p-type material. In this review we summarize some of the more important chemical and physical properties of $(CH)_x$ and its doped derivatives.

Polyacetylene, $(CH)_x$ is the simplest possible conjugated organic polymer and is therefore of special fundamental interest. Early studies on this polymer, which was known only as a dark-colored insoluble powder, concentrated on the production of pure material. Hatano *et al.*[1] found the electrical conductivity depended on the crystallinity with higher crystallinity giving higher conductivity. Berets and Smith[2] studied the effect of oxygen content on polycrystalline powder and found that oxygen in the polyacetylene affected its conductivity; the lowest oxygen content yielded the highest conductivity. Their best samples had oxygen content as low as 0.7%.

In a series of studies Shirakawa *et al.*[3-6] succeeded in synthesizing high quality polycrystalline films of $(CH)_x$ and developed techniques for controlling the *cis-trans* content. (See Figure 1).

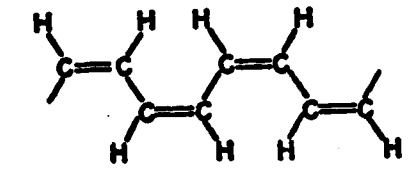

CIS

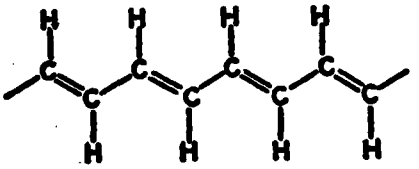

TRANS

Figure 1: Cis- and trans- polyacetylene, $(CH)_x$

The $(CH)_x$ films have a lustrous silvery appearance; they are flexible and appear to have excellent mecanical properties. Films can be made free standing, or on substrates such as glass or metal. Films have been made with thickness varying from 10^{-5} cm to 0.5 cm.

(1) SYNTHESIS OF $(CH)_x$ FILMS

Polyacetylene films may be prepared by simply wetting the inside walls of a glass reactor vessel with a toluene solution of $(C_2H_5)_3Al$ and $(n\text{-}C_4H_9O)_4Ti$ Ziegler catalyst and then immediately admitting acetylene gas at any pressure from a few centimeters up to ca 1 atmosphere pressure. The cohesive film grow on all surfaces which have been wet by the catalyst solution during a few seconds to 1 hour depending on the pressure of acetylene and temperature employed. If a polymerization temperature of ca -78°C is used, the film is formed almost completely as the cis-isomer; if a temperature of 150°C is used (decane solvent) the film is formed as the trans isomer. With room temperature polymerization the film is approxmately 80% cis-and 20% trans-isomer. If the film is carefuly washed, analytically pure $(CH)_x$ is obtained (See Table 1). The cis-isomer may be conveniently converted to the trans-isomer (the thermodynamically stable form) by heating at ca 200° for ca 1 hour.

TABLE 1

Chemical Analysis of Pure and Doped $(CH)_x$ [a]

		C%	H%	Halogen %	Total
1) $(CH)_x$	calculated	92.26	7.74		100.00
cis-$(CH)_x$	found	92.16	7.81		99.97
trans-$(CH)_x$	found	92.13	7.75		99.88
2) trans-$(CHI_{0.22})_x$ [b]	calculated	29.34	2.46	68.20	100.00
	found	29.14	2.62	68.26	100.02
3) trans-$(CHBr_{0.224})_x$ [b]	calculated	38.85	3.26	57.89	100.00
	found	38.89	3.05	58.16	100.10
3) cis-$[CH(AsF_5)_{0.099}]_x$ [b,c]	calculated	40.15	3.61	31.44	100.00
	found	39.86	3.75	31.48	99.78

[a] Galbraith Laboratories, Inc.

[b] The designation "cis" or "trans" refers to the isomeric form of the $(CH)_x$ employed in the doping experiment. It does not necessarily imply that the doped material has the same isomeric composition as the original $(CH)_x$.

[c] Arsenic: Calcd., 24.80%; Found, 24.69%.

(2) STRUCTURAL PROPERTIES OF $(CH)_x$ FILMS

Electron microscopy studies show that the as-formed $(CH)_x$ films consist of randomly oriented fibrils (typical fibril diameter of a few hundred angstroms). The bulk density is ca 0.4 gm/cm^3 compared with 1.2 gm/cm^3 as obtained by flotation techniques. This shows that the polymer fibrils fill only about one-third of the total volume. X-ray studies show that the films are polycrystalline with interchain spacing of approximately 3.8 Å.[3-6]

Characteristic infrared absorption bands of thin films can be conveniently used to distinguish the cis and trans isomers and to estimate the relative amounts of each isomer in a partly isomerized film.[3] Solid state ^{13}C nmr studies[7] have been used to confirm the assignment of a given type of film as either cis or trans. Such studies also show that isomerically pure films (within the limits of experimental error) are obtained although there is a suggestion that both types of film may contain up to ca 5% of sp^3 -hybridized carbon atoms which might be acting as cross-linking atoms between adjacent $(CH)_x$ chains.

(3) MECHANICAL PROPERTIES OF $(CH)_x$ FILMS

Fresh films of both *cis*- and *trans*-$(CH)_x$ are flexible and can be easily stretched. These properties are more pronounced with *cis* isomer films which can be stretched in a few minutes (with partial alignment of fibers) at room temperature up to 3 times their original length. Reasonably good tensile strengths (up to *ca* 3.8 kg/mm^2) are routinely obtained.

(4) STABILITY OF $(CH)_x$ FILMS

The parent $(CH)_x$ films have good thermal stability when heated in vacuum.[6] Thus, thermograms of both the *cis* and *trans* isomers show an exothermic peak at 325°C. Decomposition is rapid at this temperature. At 420°C volatile decomposition products are formed in an endothermic reaction. The parent $(CH)_x$ films slowly become brittle in air during several days and their resistance increases. However, when coated with a thin plastic film, or wax, they are stable for many weeks.

(5) ELECTRICAL PROPERTIES OF $(CH)_x$ FILMS

Shirakawa *et al.*[8] pointed out that the room temperature conductivity of crystalline films of polyacetylene depended on the *cis*-*trans* content, varying from 10^{-5} $ohm^{-1}cm^{-1}$ for the *trans* material to 10^{-9} $ohm^{-1}cm^{-1}$ for the *cis*-isomer. In view of the sensitivity of polyacetylene to impurities and/or defects as demonstrated by our doping studies,[9-16] it appears likely that the intrinsic conductivity of pure polyacetylene is even lower. This is supported by the observation that exposure of *trans*-$(CH)_x$ to the vapor of the donor, NH_3, causes the conductivity to fall more than four orders of magnitude (to $< 10^{-9}$ $ohm^{-1}cm^{-1}$) without detectable weight increase. This may be due to the coordination of the NH_3 to traces of the catalyst (which acted as a dopant). Subsequent reaction of the film with a dopant such as AsF_5, which is described in following sections, increases the conductivity many orders of magnitude to metallic levels.

From theoretical and spectroscopic studies of short chain polymers, the π-system transfer integral of $(CH)_x$ can be estimated as $\beta \simeq 2 - 2.5$ eV.[17] Thus the overall bandwidth would be of order 8-10 eV; $W = 2z\beta$, where z is the number of nearest neighbors, β is the transfer integral and W is the bandwidth in the tight-binding approximation. The electrons from the unsaturated π-system are therefore delocalized along the polymer chains. However, because of the combined effects of bond alternation and Coulomb correlation, there is an energy gap in the excitation spectrum leading to semiconducting behavior. As a result of the large overall band width and unsaturated π-system, $(CH)_x$ is fundamentally different from

either the traditional organic semiconductors made up of weakly interacting molecules (e.g., anthracene, etc.), or from other saturated polymers with monomeric units of the form 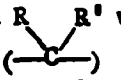 where there are no π-electrons (e.g., polyethylene, etc.). Polyacetylene is therefore more nearly analogous to the traditional inorganic semiconductors; and indeed we have shown recently that $(CH)_x$ can be chemically doped with a variety of donors or acceptors to give n-type or p-type semiconductors.[9-16]

(6) DOPING OF $(CH)_x$ FILMS

We have developed methods for doping either cis-or trans-$(CH)_x$ to p- or n-type semiconductors or metals. These methods fall into three chief categories. The silvery $(CH)_x$ films undergo very little, if any change in appearance upon doping.

(i) Exposure of the $(CH)_x$ films to a known vapor pressure of a volatile dopant e.g. I_2, AsF_5 etc. until a desired conductivity is obtained; removal of the dopant vapor at that stage then essentially "freezes" the conductivity at that value.

(ii) Treatment of the $(CH)_x$ film with a solution of the dopant in an appropriate solvent (e.g. I_2 in pentane; sodium naphthalide in THF, etc.) for a given time period.

(iii) Treatment of the $(CH)_x$ films with liquid Na/K alloy at room temperature for a few minutes to give an n-type Na/K-doped film.

A list of some doped $(CH)_x$ species is given in Table II. In addition, we have found that the following compounds also increase the conductivity of $(CH)_x$ films to either a good semiconducting or metallic range: SbF_5, SiF_4, PCl_5, PF_5, and ICN. Exact compositions and conductivities have yet to be determined.

Films doped with e.g. I_2 or AsF_5 retain their high metallic conductivity after several days exposure to air and show only a small decrease in conductivity. These films, and also those doped with e.g. Na appear to be stable in air for many weeks when coated with a protective film. In this respect it might be noted that uncoated films doped with I_2 to the metallic regime undergo essentially no change in conductivity or composition when held under water over night.

A few preliminary studies at elevated temperatures have been carried out on I_2-doped and AsF_5-doped films. Films containing the former dopant appear to retain their semiconducting properties up to

TABLE 2

Conductivity of Polycrystalline Polyacetylene and Derivatives (As-Grown Films)[a]

Material	Conductivity $\sigma(ohm^{-1}cm^{-1})(25^{\circ}C)$
cis-$(CH)_x$ [b]	1.7×10^{-9}
trans-$(CH)_x$ [b]	4.4×10^{-5}
trans-$[(CH)(HBr)_{0.04}]_x$	7×10^{-4}
trans-$(CHCl_{0.02})_x$	1×10^{-4}
trans-$(CHBr_{0.05})_x$ [b]	5×10^{-1}
trans-$(CHBr_{0.23})_x$	4×10^{-1}
cis-$[CH(ICl)_{0.14}]_x$	5.0×10^{1}
cis-$(CHI_{0.25})_x$	3.6×10^{2}
trans-$(CHI_{0.22})_x$ [b]	3.0×10^{1}
trans-$(CHI_{0.20})_x$	1.6×10^{2}
cis-$(CHI_{0.28})_x$	5.0×10^{2}
cis-$[CH(IBr)_{0.15}]_x$	4.0×10^{2}
trans-$[CH(IBr)_{0.12}]_x$	1.2×10^{2}
trans-$[CH(AsF_5)_{0.03}]_x$ [b]	7×10^{1}
trans-$[CH(AsF_5)_{0.10}]_x$	4.0×10^{2}
cis-$[CH(AsF_5)_{0.14}]_x$	5.6×10^{2}
trans-$[Na_{0.28}(CH)]_x$	8×10^{1}

(a) The prefix "cis" or "trans" refers to the isomeric composition of the $(CH)_x$ which was used in a given doping experiment.

(b) Composition obtained by chemical analysis from Galbraith Laboratories, Inc. (Sum of all elements ~ 99.8-100.1%).

at least ca 100°C whereas films involving AsF_5 remain semiconducting up to at least 150°-200°C.

(7) ELECTRICAL CONDUCTIVITY OF DOPED $(CH)_x$ FILMS AND SEMICONDUCTOR-METAL TRANSITION

When pure polyacetylene is doped with a donor or an acceptor, the electrical conductivity increases sharply over many orders of magnitude at low concentration, then saturates at higher dopant

levels, above approximately 1%.[9-16] The maximum conductivity we have reported to date at room temperature for nonaligned cis-$[CH(AsF_5)_{0.14}]_x$ was 560 $ohm^{-1}cm^{-1}$. The typical behavior for the conductivity as a function of dopant concentration (y) is shown in Figure 2. The general features appear to be the same for the various donor and acceptor dopants, but with detailed differences in the saturation values and the critical concentration at the "knee" in the curve (above which σ is only weakly dependent on y). These transport studies suggest a change in behavior near 1% dopant concentration; a semiconductor to metal transition.

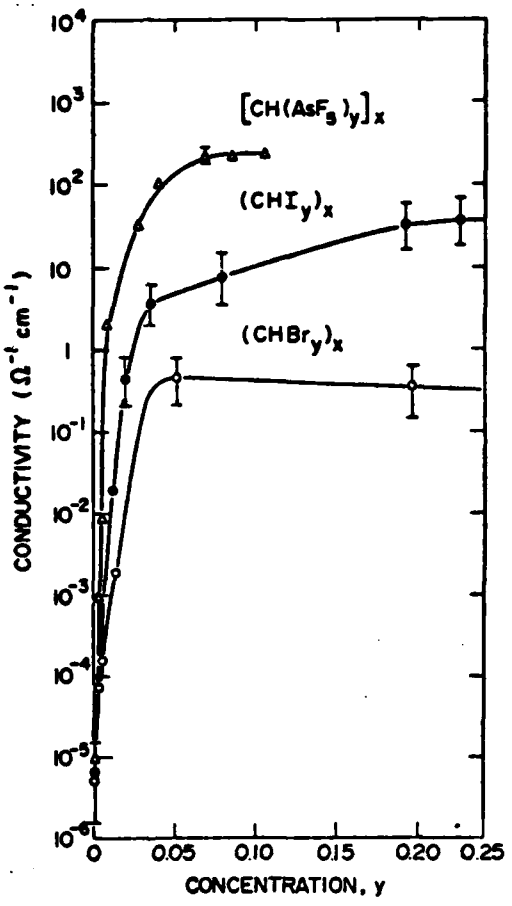

Figure 2: Electrical conductivity (room temperature) as a function of dopant concentration.

To verify the existence of the semiconductor-to-metal transition, far infrared transmission data were taken[10] on samples of varying concentrations of iodine and AsF_5 (with qualitatively similar results). The data for a series of iodinated samples are shown in Figure 3 for y = 0.0, 0.9, 2.0 and 6.0 at%. In the case of the 6% sample, there is no observable transmission throughout the ir down to 20 cm^{-1} implying a continuous excitation spectrum; i.e., metallic. For the 2% sample, the transmission was zero at the high end of the spectrum (4000 cm^{-1} to 300 cm^{-1}), but increases below 300 cm^{-1} to about 60% by 40 cm^{-1} implying an energy gap at low frequencies. The far ir transmission through the 0.9% sample is near 90% with no significant change from an undoped sample. The inset to Figure 3 shows the absorption coefficient, α, (uncorrected for reflection) at 40 cm^{-1} as a function of dopant concentration. The transition is sharp with a critical concentration (n_c) in the range 2-3%. Similar results have been obtained with AsF_5 although n_c appears to be slightly smaller. The values for n_c as inferred from the ir and dc transport measurements are in agreement.

As an initial point of view we treated this transition as similar to that seen in heavily doped semiconductors. In this case, one expects the halogen and AsF_5 dopants to act as acceptors with

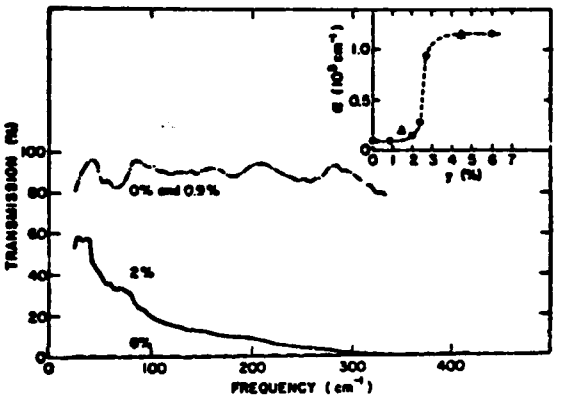

Figure 3: Far infrared (20 cm^{-1} to 400 cm^{-1}) transmission of I_2-doped polyacetylene (sample temperature was 77 K). The inset shows the absorption coefficient (uncorrected for reflection) at 40 cm^{-1} vs. concentration (solid points, trans-polymer; triangles, cis-polymer).

localized hole states in the gap, with the hole bound to the acceptor in a hydrogen-like fashion. For low concentrations, one expects the combination of impurity ionization and variable range hopping to lead to a combination of activated processes as observed experimentally. However, as extensively discussed by Mott[18] and others,[19] if the concentration is increased to a critical level, then the screening from carriers will destroy the bound states giving an insulator-to-metal transition. This will occur when the screening length becomes less than the radius of the most tightly bound Bohr orbit of the hole and acceptor in the bulk dielectric;

$$n_c^{1/3} \simeq (4a_H)^{-1} \left(\frac{m^*}{m\epsilon}\right)$$

where a_H is the Bohr radius, ϵ is the dielectric constant of the medium and m^*/m is the ratio of the band mass to the free electron mass. Assuming $m^*/m \simeq 1$ and using $\epsilon \simeq 8$ from ir reflection measurements, we estimate $n_c \sim 10^{20} - 10^{21}$ cm^{-3}. Since the density of carbon atoms is about 2×10^{22} cm^{-3}, n_c would be in the range of a few percent assuming one carrier per dopant. The good agreement with our experimental results is probably fortuitous in view of the much over-simplified model. However, the overall features of the semiconductor-metal transition at high doping levels are very similar to those observed in traditional inorganic semiconductors.

(8) THE ENERGY GAP AND ABSORPTION SPECTRUM

For the undoped polymer, the absorption edge (see Figure 4) is quite sharp, rising much more rapidly than the typical three-dimensional (3d) joint density of states, which increases from the gap edge as $(\epsilon - E_g)^{\frac{1}{2}}$. In contrast, if we assume weak interchain coupling as suggested above, the 1d joint density of states has the well-known $(\epsilon - E_g)^{-\frac{1}{2}}$ singularity at the gap edge with a correspondingly steep absorption edge. Actual attempts to fit with a Gaussian broadened 1d density of states resulted in good agreement with the data near the gap edge. The magnitude of the absorption maximum ($\alpha \sim 3 \times 10^5$ cm^{-1}) is comparable to that for interband transitions in more common direct gap semiconductors.[20] A precise value for the energy gap requires a detailed theoretical model. If we assume a 1d band structure with broadened 1d density of states, $E_g = E_{max} = 1.9$ eV. Using the more conventional definition of the onset of absorption, one estimates $E_g \simeq 1.4 - 1.6$ eV.

These values are considerably larger than the activation energy obtained from temperature dependent resistivity studies of *trans*-$(CH)_x$ (0.3 eV).[8] This is consistent with the transport in undoped $(CH)_x$ being dominated by trace impurities or defects.[9-15]

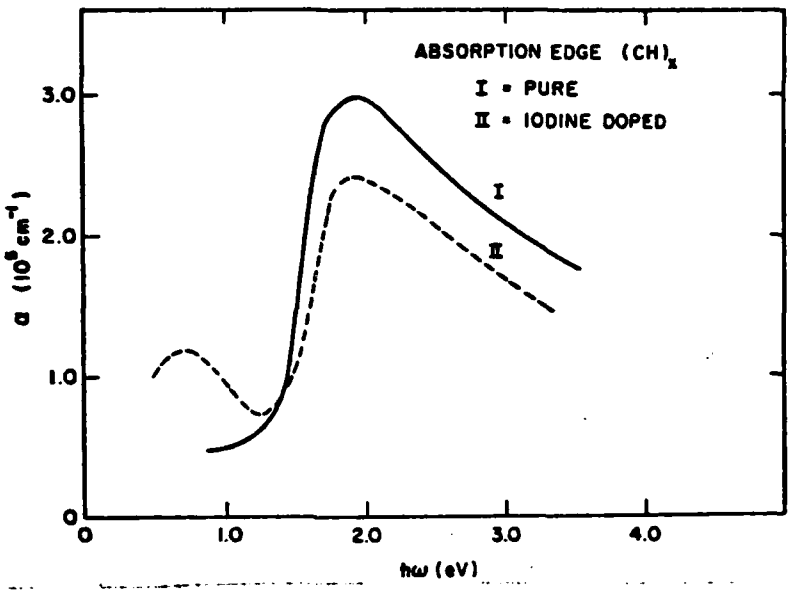

Figure 4: Absorption coefficient of trans-$(CH)_x$ before and after doping to saturation as a function of frequency; film thickness 0.1 μm.

Ovchinnikov[17] has argued that the energy gap extrapolated to infinite chain polyenes is too large to be accounted for by simple band theory of the bond-alternated chain, and he therefore concluded that Coulomb correlations play an important role. In a tight binding calculation, the band gap due to bond alternation would be $\delta\beta = \delta x \left.\frac{\partial\beta}{\partial x}\right|_{x_o} = \frac{\delta x}{a}\beta(x_o)$ where δx is the difference in bond lengths and x_o the average bond length; $\beta(x) = \beta_o \exp(-x/a)$ is the transfer integral where a is a characteristic atomic distance ($a \sim 0.7$ Å) describing the fall-off of the carbon $2p_\pi$ wavefunction ($\beta(x_o) \simeq 2.5$ eV). If we assume δx takes the maximum value, equal to the difference in bond lengths between a single bond (1.51 Å as in ethane) and a double bond (1.34 Å as ir ethylene) we estimate $E_g \simeq 0.6$ eV. Certainly this question must be resolved with more detailed band calculations.[21] However, based on results obtained thus far in our transport[9-15] and magnetic[22] studies of $(CH)_x$, we see no experimental evidence suggesting strong Coulomb correlations.

The absorption spectra after doping with iodine is shown in Figure 4, similar results are obtained after doping with AsF_5. There is relatively strong absorption at low frequencies within the

gap as would be expected for a heavily doped semiconductor. Detailed studies of the onset of absorption within the gap at lightest doping levels are in progress. More important in the context of this study is the observation that the strong interband transition persists even at the highest doping levels. This result suggests that at least for these dopants the basic π-electron band structure of $(CH)_x$ remains intact in the doping process, consistent with the charge transfer doping model[11,12] with A^- species between chains. An uninterrupted π-system is consistent with the excellent transport properties of metallic doped $(CH)_x$. On the other hand recent studies[23] with bromine doping have revealed a major change in the absorption spectrum after doping, consistent with earlier observations[12] that bromine tends to add to the double bond (at least at high concentrations) with a corresponding decrease in conductivity. Studies must be carried out with a variety of dopants before general conclusions can be drawn.

Throughout the above discussion we have assumed that the absorption edge results from an interband transition with the creation of electron-hole pairs. The possibility of electron-hole bound states (excitons) on the chain must be considered since such exciton transitions can lead to a sharp absorption edge below the gap. However, the observation of this absorption even at the highest doping levels argues against a transition to an exciton bound state, which would be screened in the metal. Moreover, early photoconductivity measurements[24] on powder samples suggest a photo-conductive edge consistent with the absorption edge.

(9) ORIENTED FILMS: ANISOTROPIC ELECTRICAL PROPERTIES[14]

The high conductivity in the metallic state above n_c (see Figure 2) is particularly interesting since electron microscopy studies[5,6] show that the $(CH)_x$ films consist of tangled randomly oriented fibrils (typical fibril diameter of a few hundred angstroms). The bulk density[6] is 0.4 gm/cm^3 compared with 1.2 gm/cm^3 as obtained by flotation techniques, indicating that the polymer fibrils fill only about one-third of the total volume. X-ray studies[5] show that the $(CH)_x$ films are polycrystalline with interchain spacing of approximately 3.8 Å. Consequently we expect the interchain electronic transfer integrals to be small, $\sim$ 0.1 eV, i.e., less than or comparable to the intermolecular transfer integrals along the b-axis in TTF-TCNQ where the intermolecular spacing is 3.6 Å. On the other hand, molecular spectroscopic studies of short chain polymers lead to the conclusion that the intrachain transfer integrals for carbon atoms separated by $\sim$ 1.4 Å are of order 2 - 2.5 eV. Thus we anticipate a highly anisotropic band structure with correspondingly anisotropic transport in $(CH)_x$. Indirect evidence of this was obtained from the temperature dependence of the conductivity in $(CH)_x$ doped to concentrations above the semiconductor-

to-metal transition.[9-15] The conductivity was found to decrease on lowering the temperature in a manner similar to that observed in polycrystalline $(SN)_x$[25], sublimed films of $(SN)_x$[25] or polycrystalline TTF-TCNQ where the transport is limited by a combination of anisotropy and interparticle contact. In these cases, the conductivity decreases even though the single crystal transport measurements along the principal conducting axis clearly imply metallic behavior.

It is well known that many polymers can be stretch-oriented by mechanical elongation. Shirakawa and Ikeda have recently reported[27] significant orientation of $(CH)_x$ after stretch elongation; they have been able to vary the amount of orientation by combined mechanical and thermal treatment resulting in elongation with $\ell/\ell_o \sim 1$ to 3 where ℓ is the final stretched length and ℓ_o is the unstretched length.

The room temperature results on partially oriented films are summarized in Figures 5 and 6.[14] The anisotropy is plotted in Figure 5 as a function of dopant concentration for $\ell/\ell_o = 2.1$ and $\ell/\ell_o = 2.9$. The induced anistropy of the undoped oriented films appears to increase approximately as the square of the elongation (prior to stretching the non-aligned samples are isotropic both before and after doping with AsF_5). The anisotropy remains after doping, increasing modestly with iodine and more steeply with AsF_5. The effects of elongation (alignment) on the absolute values of $\sigma_{\parallel}$ and $\sigma_{\perp}$ are shown on Figure 6 for the heavily doped metallic polymer $[CH(AsF_5)_{0.10}]_x$. The parallel conductivity increases dramatically with alignment; the solid curve follows $\sigma = \sigma_o (\ell/\ell_o)^2$ where $\sigma_o = 300$ ohm^{-1}cm^{-1}.

Scanning electron microscope pictures of the films as grown and after stretch alignment are shown in Figures 7 and 8 respectively. The characteristic branched and twisted fibrils of the unstretched polymer discussed earlier by Ito *et al.*[5,6] are clearly visible in Figure 7. Elongation results in partial alignment as shown in Figure 8. However comparison of the two shows that the fractional alignment is only modest.

The temperature dependence of the parallel and perpendicular conductivities and the anisotropy for an oriented film ($\ell/\ell_o = 2.9$) doped into the metallic regime with AsF_5 are shown in Figure 9. The solid points result from four probe measurements on two separate ($\parallel$ and $\perp$) films; the x points result from the Montgomery measurements. The three samples were taken from the same initial film and doped simultaneously to a final composition $[CH(AsF_5)_{0.10}]_x$. We expect the Montgomery technique to give the more reliable data since the measurements were taken on a single sample. The four-probe data come from two separate samples ($\parallel$ and $\perp$), so that slightly different final compositions are possible. Nevertheless, the results from the two independent sets of measurements are

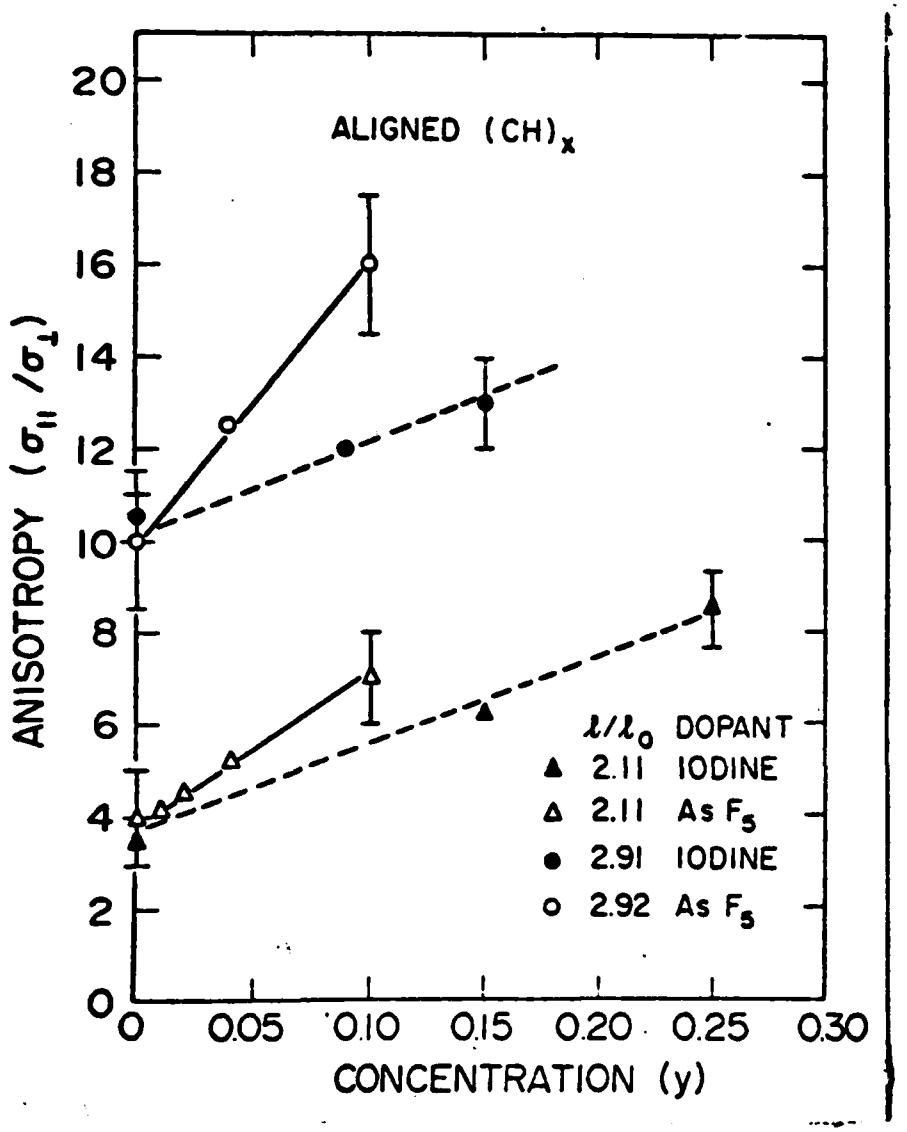

Figure 5: The electrical anisotropy, $\sigma_{\parallel} / \sigma_{\perp}$ as a function of dopant concentration for partially aligned $(CH)_x$ films at different values of elongation (ℓ/ℓ_0).

consistent, and the general agreement is excellent. The room temperature parallel conductivity is in excess of 2000 $ohm^{-1}cm^{-1}$; the average of the two measurements yields 2150 $ohm^{-1}cm^{-1}$. On cooling, $\sigma_{\parallel}$ and $\sigma_{\perp}$ decrease slowly; however, the conductivity remains high even at the lowest temperatures, consistent with metallic behavior.

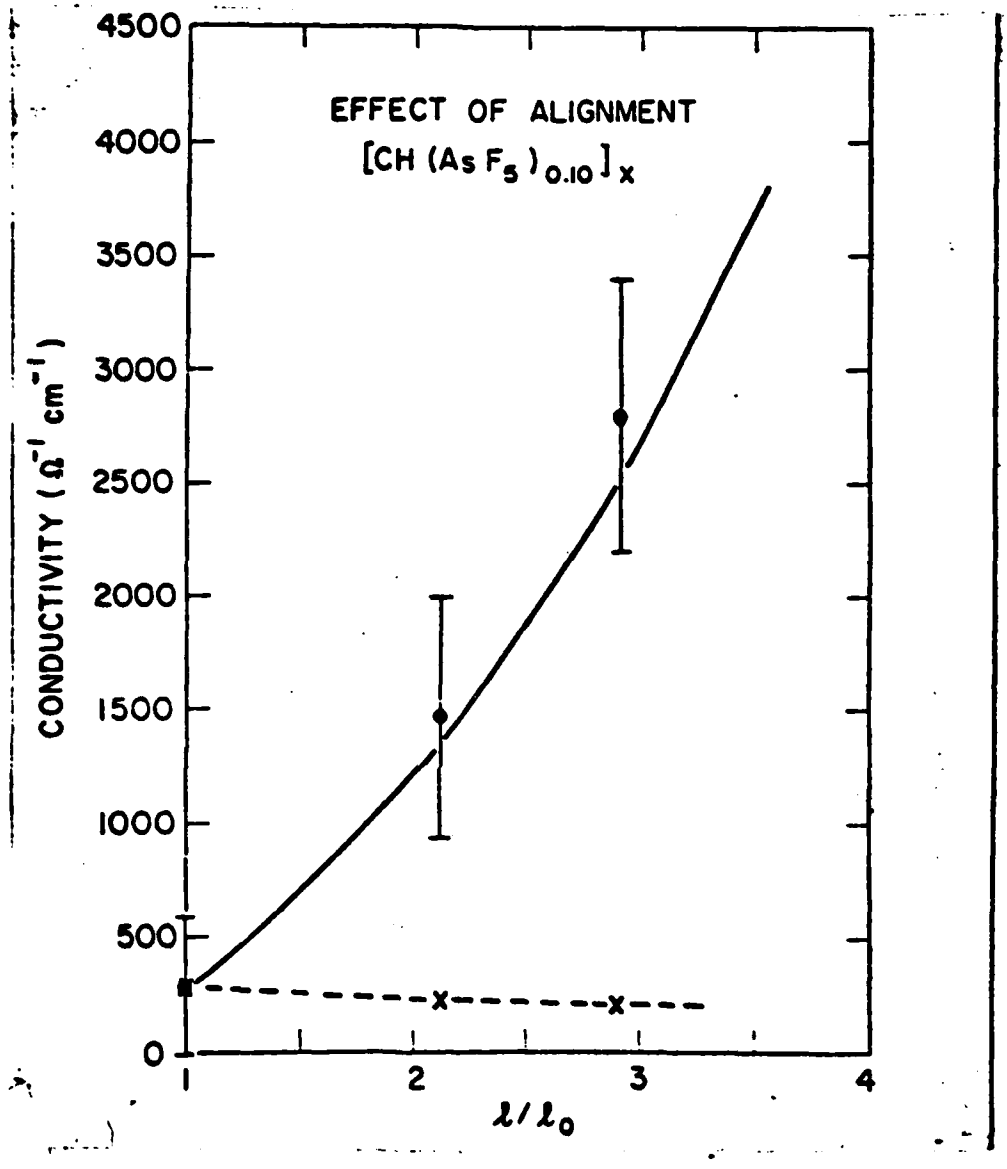

Figure 6: Conductivity of metallic, heavily-doped $[CH(AsF_5)_{0.10}]_x$ as a function of elongation (l/l_0) as obtained by Montgomery method.

• • • parallel to alignment direction

x x x perpendicular to alignment direction

Figure 7: Scanning electron microscope picture of as-grown $(CH)_x$. (The average fibril diameter is approximately 200 Å.)

Figure 8: Scanning electron microscope picture of stretch oriented $(CH)_x$. (The average fibril diameter is approximately 200 Å.)

A more detailed examination of the data shows that $\sigma_{\parallel}$ remains approximately constant, increasing slightly (~0.5%) down to 260 K, whereas $\sigma_{\perp}$ decreases monotonically.

The results of these initial studies on oriented $(CH)_x$[14] must be compared with earlier results on the random polymer.[9-13] The general conclusion is that the transport is indeed limited by a combination of interparticle contact and anisotropy even in the partially oriented films; the intrinsic conductivity along the $(CH)_x$

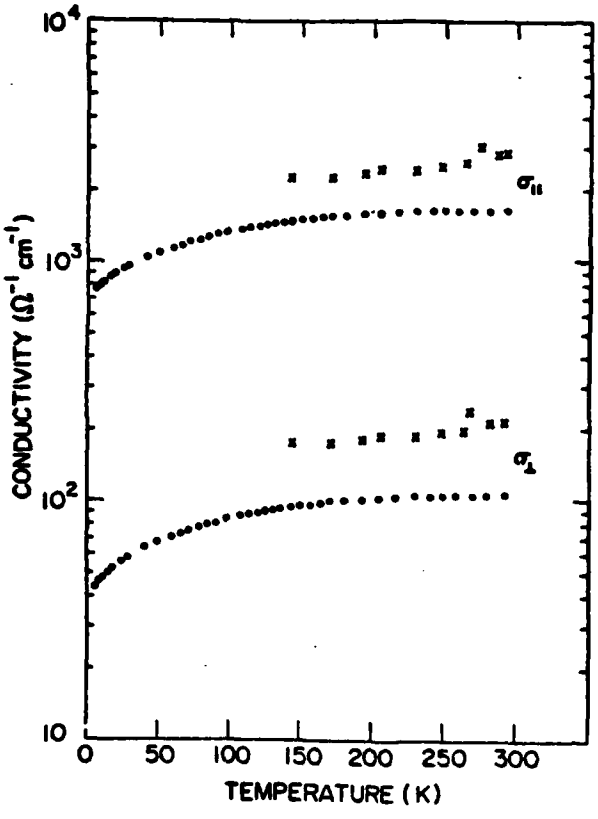

Figure 9: Conductivity vs. temperature for oriented $[CH(AsF_5)_{0.10}]_x$. The film was stretch-oriented ($l/l_o = 2.9$) prior to doping.

• • • four-probe measurements
x x x Montgomery measurements

chain direction in the doped metallic polymer is much higher than the measured value. The trends in the data together with the electron microscope photographs suggest that better orientation will lead to considerable enhancement of the anisotropy and the absolute room temperature conductivity (Figure 5) with $\sigma_{\parallel}$ vs. (T) probably increasing substantially on cooling.

(10) ORIENTED FILMS: ANISOTROPIC OPTICAL PROPERTIES[15]

Direct visual inspection of oriented $(CH)_x$ films reveals a

silvery reflection, similar to Al foil, but somewhat darker. Through a polarizer, the reflection polarized parallel to the fiber and polymer chain orientation direction is silvery, but the reflection polarized perpendicular is pastel orange. Doping with AsF_5 ($\sigma_{\parallel} \geq 10^3$ $(\text{ohm}^{-1}\text{cm})^{-1}$ produced no obvious change by direct vision on parallel polarization, but the reflection polarized perpendicular became much darker indicative of increased anisotropy on doping.

The reflectance results are shown in Figures 10 and 11. For the pristine sample, $R_{\parallel}$ data show a broad maximum that corresponds to the absorption peak near 2 eV. $R_{\parallel}$ decreases in the infrared consistent with a semiconductor picture; extrapolation of the low energy data suggests a low frequency reflectance of 12 to 18% implying a dielectric constant, $\epsilon_{\parallel}(o) \simeq 5$. The perpendicular reflectance is flat (~4%, $\epsilon_{\perp}(o) \simeq 2$) at low frequencies, with a weak maximum centered at 1.7 eV. At higher frequencies $R_{\perp}$ falls proportionately faster than $R_{\parallel}$ suggesting that the observed structure in $R_{\perp}$ is intrinsic and not the result of incomplete orientation. The optical anisotropy goes through a minimum of $(R_{\parallel}/R_{\perp}) = 4.7$ at 1.65 eV, increases to $(R_{\parallel}/R_{\perp}) \simeq 10$ at 2.5 eV, then decreases at higher energy.

Heavy doping of the sample with AsF_5 ($\sigma_{\parallel} \geq 10^3$ $\text{ohm}^{-1}\text{cm}^{-1}$) increases $R_{\parallel}$ below 1.4 eV (Figure 11); the low frequency results are similar to the free carrier reflectance in heavily doped semiconductors. The trans-$(CH)_x$ maximum near 2 eV remains after doping, consistent with the absorption results described earlier. The overall result is an increase of the optical anisotropy at all energies below 2.5 eV.

A somewhat more quantitative comparison of the absorption and $R_{\parallel}$ reflectance of the undoped polymer can be made by modeling the interband transition as a single Lorentz oscillator centered at 2 eV. Thus, assuming

$$\epsilon(\omega) = 1 + \frac{\Omega_0^2}{\omega_g^2 - \omega^2 - i\omega\Gamma}$$

leads to $E_g = \hbar\omega_g = 2$ eV, $\hbar\Omega_0 \simeq 4.0$ eV and $\hbar\Gamma \simeq 0.54$ eV; the latter two parameters being determined by fitting to $\epsilon_{\parallel}(o)$ and $R_{\parallel}(2\text{ eV})$. From these one estimates a peak absorption at 2 eV of $\alpha \simeq 5 \times 10^5$ cm^{-1} in good agreement with Figure 4. More detailed comparison must await a Kramers-Kronig analysis of the full reflectance spectrum. Note, however, that the implied quantitative agreement between the $R_{\parallel}$ data from partially aligned films of undoped $(CH)_x$ (Figure 10) and the absorption by non-aligned films (Figure 4) implies that the strong absorption is polarized along the chain direction. We therefore conclude that the anisotropy is intrinsic and is present on a single fiber scale in the non-oriented polymer. The large optical anisotropy is consistent with a quasi-(1d) band

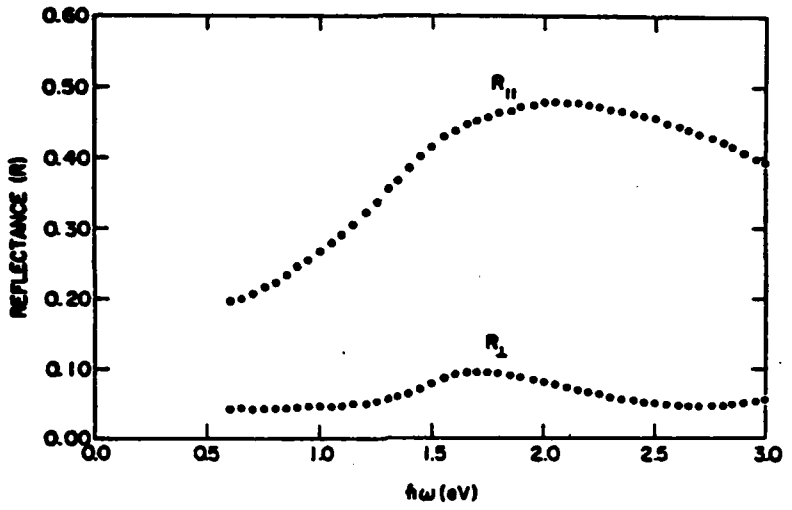

Figure 10: Anisotropic reflectance from partially oriented film of $(CH)_x$ ($\ell/\ell_o = 2.94$).

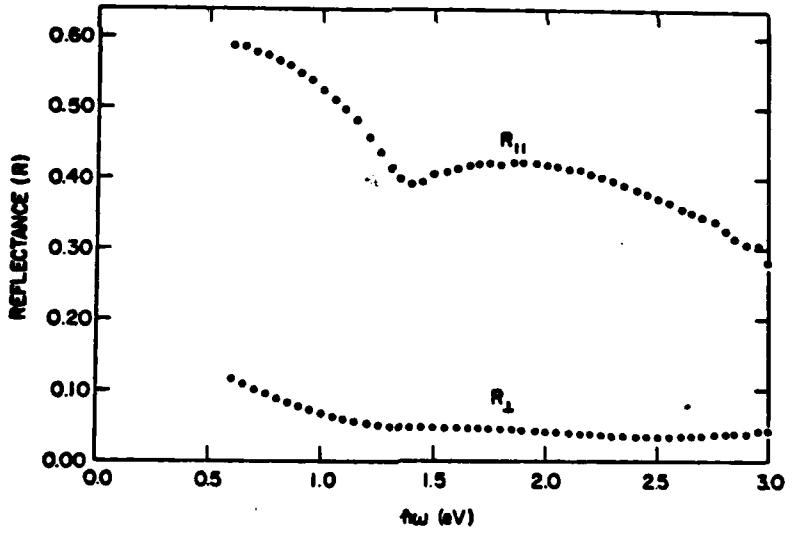

Figure 11: Anisotropic reflectance from partially oriented film of $(CH)_x$ ($\ell/\ell_o = 2.94$) after doping with AsF_5 ($\sigma_{\parallel} = 10^3$ ohm^{-1}cm^{-1}).

structure as described above.

The effect of doping on the reflectance is entirely consistent with the previous interpretation of a metal-semiconductor transition in doped polyacetylene.[9-15] The interband transition remains visible, but the reflectance begins to rise at lower frequencies due to the free carrier contribution to the dielectric function. Detailed Drude fits require extension of the data into the far ir. These studies are presently being carried out.

(11) SEMICONDUCTOR PHYSICS OF $(CH)_x$ FILMS: COMPENSATION AND JUNCTION FORMATION[13]

A series of experiments have been reported which demonstrate that donors or acceptors can dope polyacetylene to n-type or p-type respectively, and that the two kinds of dopants can compensate one another.[13] The formation of a rectifying p-n junction as well as Schottky barrier junctions have been demonstrated. These results suggest the possibility of utilizing doped polyacetylene in a variety of potential semiconductor device applications; in particular those involving solar cell applications.

Compensation of n-type material by subsequent acceptor doping has been successfully demonstrated using Na (donor) and iodine or AsF_5 (acceptors). Figure 12 shows the compensation of Na-doped polyacetylene by iodine. The Na-doped films were prepared by treating the polymers with a solution of sodium naphthalide, $Na^+(C_{10}H_8)^-$, in THF whereupon electron transfer from the naphthalide radical anion to the $(CH)_x$ occurred. In each case the pure cis-polyacetylene was first doped with sodium until the conductivity was in the saturation range. Subsequent exposure to iodine vapor resulted in the compensation curve plotted in Figure 12. The compensation proceeds more slowly than the original doping; the electrical conductivity of the n-type sample gradually decreases and reaches a minimum. Continued doping with iodine results in conversion to p-type material with an associated increase in conductivity. Similar compensation has been achieved with AsF_5 as the acceptor.

Starting with an initial composition $(CHNa_{0.27})_x$, the compensation point with iodine occurred at $(CHNa_{0.27}I_{0.28})_x$; all compositions being determined by measurement of weight increase. Thus the compensation point corresponds approximately to a stoichiometric sodium to iodine ratio consistent (within the limits of error) to the presence of equal concentrations of Na^+ and I^- in the compensated polymer. Continued doping leads to p-type material, where the iodine is known to be present as I_3^- from Raman studies.[26,27]

The assignment of donor doped material as n-type and acceptor doped material as p-type follows from the chemical properties of the

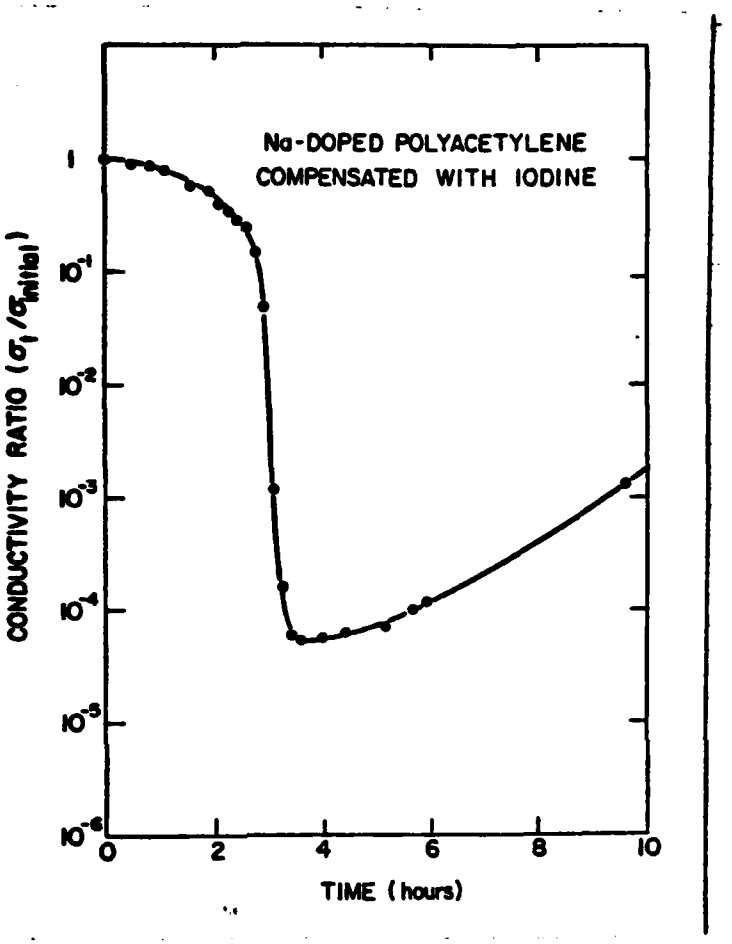

Figure 12: Compensation curve for Na-doped polyacetylene; conductivity ratio ($\sigma_{(t)}/\sigma_{initial}$) vs. time. The sample was initially doped n-type and subsequently exposed to iodine vapor.

donor and acceptor dopants. Moreover, the assignments are consistent with the results obtained from studies of graphite intercalated with alkali metals and iodine or AsF_5 respectively.[28] Finally, thermoelectric power measurements on acceptor doped $(CH)_x$ yield a positive Seebeck coefficient consistent with p-type material. Moreover, the value of +15 μV/K found at room temperature for $(CH)_x$ heavily doped with AsF_5 is consistent with metallic behavior. Initial experiments directed toward fabrication of p-n junctions are encouraging as shown in Figure 13. The junction was made by mechanically pressing together n-type (Na-doped) and p-type (AsF_5 - doped) strips of polymer film. Although some hysteresis is evident, a typical diode characteristic is seen in the I-V curve. Junctions have also been

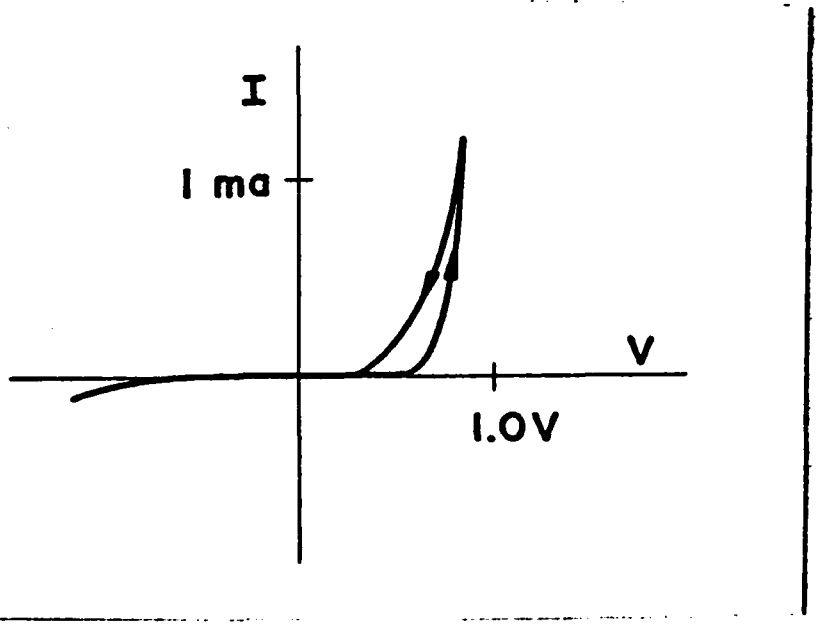

Figure 13: I-V curve for a doped polyacetylene p-n junction.

made using a single polymer strip doped n-type on one-half and p-type on the other half. Note that in all cases the forward bias direction was consistent with the p-type and n-type character of the acceptor and donor doped material.

Initial experiments directed toward fabrication of Schottky barrier rectifying diodes have also provided encouraging results. Both n-type material (e.g. Pt metal in contact with $[CH(Na)_y]_x$) and p-type material (e.g. Na metal in contact with $[CH(AsF_5)_y]_x$) can be used to obtain typical diode characteristics such as that shown in Figure 14. Experiments to date have utilized point contact geometry. More work is needed in order to elucidate the nature of the interface, since, as shown in Figure 12, compensation has been demonstrated and a possible chemical reaction may occur at the interface between Na and the $[CH(AsF_5)_y]_x$.

(12) ELECTRICAL PROPERTIES OF DOPED $(CH)_x$ FILMS

At relatively low doping levels, the conductivity is activated as shown for example in Figure 15 for $(CHI_y)_x$ (similar data have been obtained for AsF_5, Br etc.) where the conductivity is plotted vs. 1/T on a semilog scale. In general, we find that the conductivity of doped polyacetylene decreases with decreasing temperature. However, the plot of $\ell n\sigma$ vs. 1/T do not give straight line behavior as seen in Figure 15. Plotting the data as $\ell n\sigma$ vs. $T^{-\frac{1}{4}}$ (or $T^{-\frac{1}{2}}$)

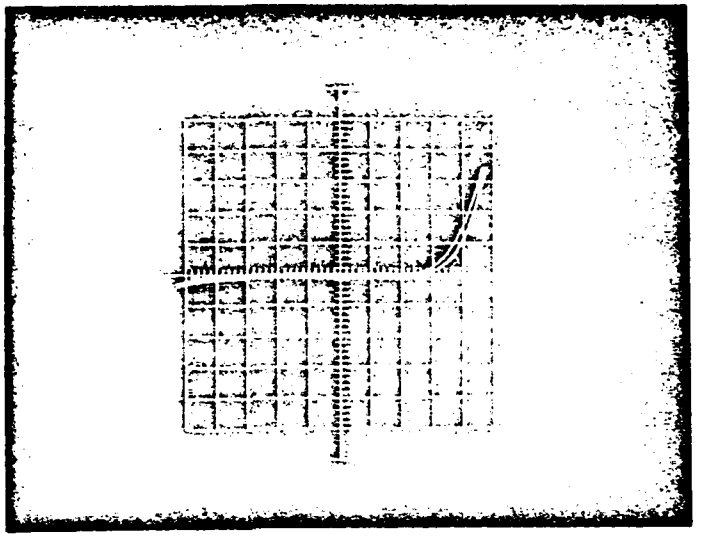

Figure 14: Oscilloscope picture of I vs. V for Schottky barrier diode; Na contact on AsF_5-doped $(CH)_x$.
x = 0.5 V/division; y = 1 μA/division at 60 Hz.

tends to give more nearly straight line behavior as shown in Figure 16. Again this behavior is typical of that observed in non-crystalline inorganic semiconductors such as amorphous Si, although $(CH)_x$ films are at least partially crystalline as demonstrated by X-ray diffraction. The twisted fibril structure of the films, (see Figure 7) indicates the presence of significant disorder.

The general behavior shown on Figures 15 and 16 is toward smaller activation energy as the dopant concentration increases. We use the initial slope of the 1/T plots to determine the approximate thermal activation energy, E_o, which serves as a simple index of the conductivity behavior. The resulting activation energies are shown in Figure 17 as a function of concentration y for both $(CHBr_y)_x$ and $(CHI_y)_x$. Undoped polyacetylene has an activation energy in the range from 0.3 eV (trans) to 0.5 eV (cis).[6] However, the compensation experiments indicate that the conductivity in the undoped polymer results from residual defects and/or impurities.[9-11] Thus the intrinsic $(CH)_x$ activation energy is significantly higher, in agreement with the optical studies (Figure 4). On doping with halogen, the activation energy drops rapidly reaching a value as low as 0.018 eV at about 20 mole % iodine. Similar results are obtained

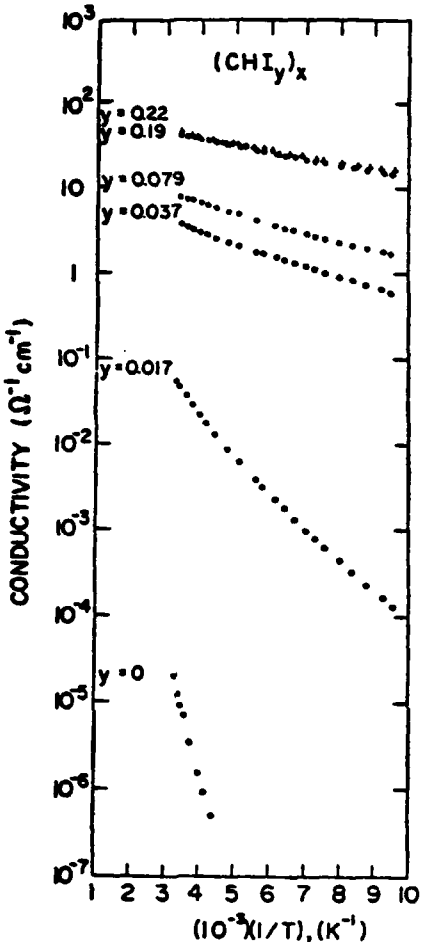

Figure 15: $\ln\sigma$ vs. $1/T$ for $(CHI_y)_x$ for various concentrations (y) of iodine.

from the bromine doping.

The sudden change in the concentration dependance of the conductivity and the activation energy near y = 0.02 is consistent with a semiconductor-to-metal transition near the 2% dopant level, in agreement with earlier far infrared and transport studies.[10] The temperature dependence studies indicate that samples with y < 0.02

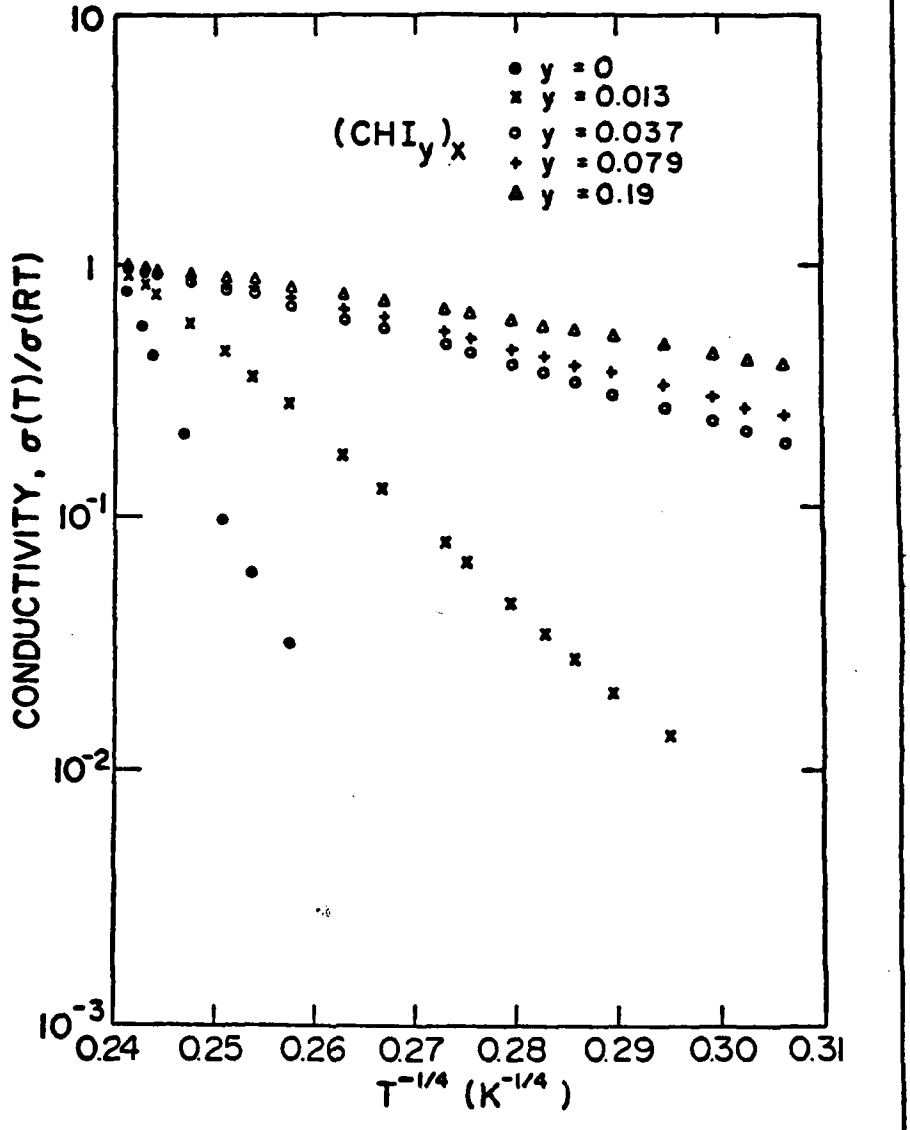

Figure 16: $\ln\sigma$ vs. $1/T^{\sim}$ for $(CHI_y)_x$ with various concentrations of iodine.

show an activated conductivity with the activation energy being a strong function of dopant concentration. For $y > 0.02$, the activation energy is sufficiently small that interfibril contacts in the polycrystalline polymer films are playing a limiting role.

The mobility of the heavily doped non-oriented polymer in the

metallic regime, was estimated to be about 1 cm^2/Volt-sec.[10] This value was subsequently confirmed by Hall effect measurements.[29] However as demonstrated above, the transport is limited by the interfibril contact; the intrinsic mobility is undoubtedly considerably higher. Initial utilization of polymer processing techniques to orient the polymer fibrils have resulted in significant improvement of the conductivity as shown in Figure 6.[14] Using the higher conductivity of these partially oriented films to estimate the mobility leads to a value of order 5-10 cm^2/Volt-sec; this clearly is a lower limit.

In conclusion, as can be seen from the following list of conductivities of common substances, $(CH)_x$ is quite remarkable in that its conductivity can be readily modified to span an extraordinarily large range. Considering possible polyacetylene derivatives, replacement of some or all of the hydrogen atoms in $(CH)_x$ with organic or inorganic groups, copolymerization of acetylene with other acetylenes or olefins, and the use of different dopants should lead to the development of a large new class of conducting organic polymers with electrical properties that can be controlled over the full range from insulator to semiconductor to metal.

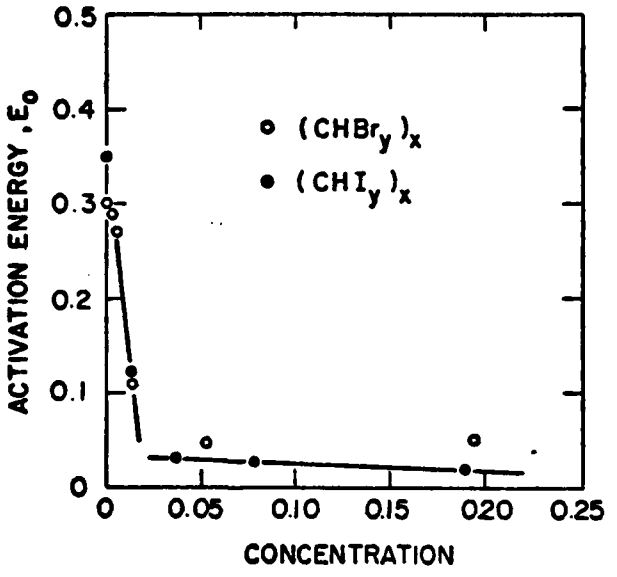

Figure 17: Activation energy of halogen-doped polyacetylene as a function of concentration. The activation energies were obtained from the slopes of the curves in Figure 15.

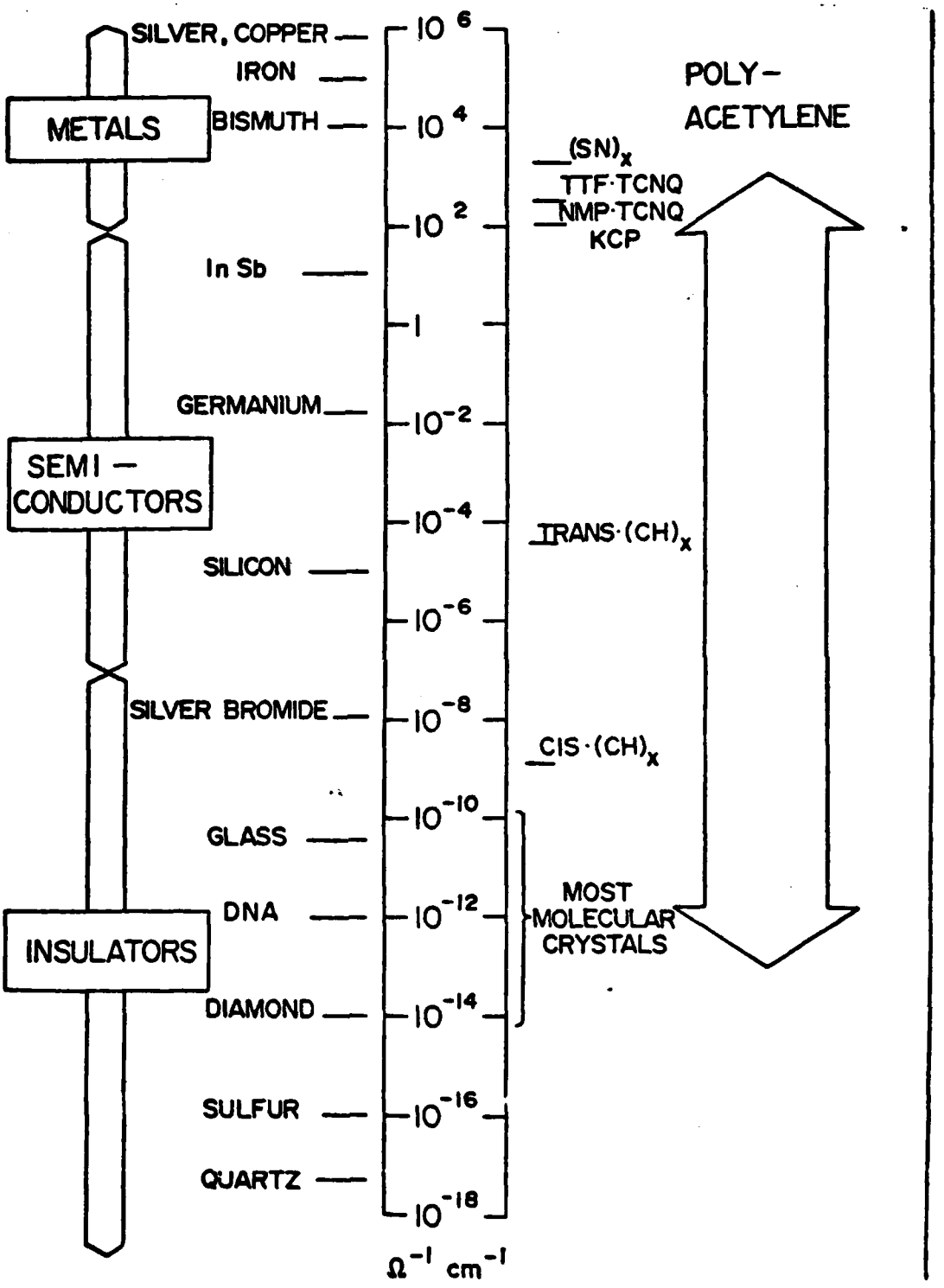
METALS
SEMI – CONDUCTORS
INSULATORS
SILVER, COPPER
IRON
BISMUTH
In Sb
GERMANIUM
SILICON
SILVER BROMIDE
GLASS
DNA
DIAMOND
SULFUR
QUARTZ
10^{6}
10^{4}
10^{2}
1
10^{-2}
10^{-4}
10^{-6}
10^{-8}
10^{-10}
10^{-12}
10^{-14}
10^{-16}
10^{-18}
Ω^{-1} cm^{-1}
$(SN)_x$
TTF·TCNQ
NMP·TCNQ
KCP
TRANS·$(CH)_x$
CIS·$(CH)_x$
MOST MOLECULAR CRYSTALS
POLY-ACETYLENE

ACKNOWLEDGMENTS

The authors are indebted to the following persons for their important contributions to the work described in this review: Dr. Hideki Shirakawa (Tokyo Institute of Technology); C. K. Chiang, M. A. Druy, C. R. Fincher, Jr., S. C. Gau, E. J. Louis, Y. Matsumura, Y. W. Park, D. L. Peebles and A. Pron. This work was supported by the Office of Naval Research.

REFERENCES

1. M. Hatano, S. Kambara, S. Okamoto, J. Polym. Sci. 51, 526 (1961).
2. D. J. Berets and D. S. Smith, Trans. Faraday Soc. 64, 823 (1968).
3. H. Shirakawa and S. Ikeda, Polym. J. 2, 231 (1971).
4. H. Shirakwa, T. Ito and S. Ikeda, Polym. J. 4, 460 (1973).
5. T. Ito, H. Shirakawa and S. Ikeda, J. Polym. Sci. Polym. Chem. Ed. 12, 11 (1974).
6. T. Ito, H. Shirakawa and S. Ikeda, J. Polym. Sci. Polym. Chem. Ed. 13, 1943 (1975).
7. M. M. Maricq, J. S. Waugh, A. G. MacDiarmid, H. Shirakawa and A. J. Heeger, J. Amer. Chem. Soc., (in press) (1978).
8. H. Shirakawa, T. Ito, S. Ikeda, Die Macromoleculare Chemie, (in press) (1978).
9. H. Shirakawa, E. J. Louis, A. G. MacDiarmid, C. K. Chiang and A. J. Heeger, Chem. Comm. 578 (1978).
10. C. K. Chiang, C. R. Fincher, Jr., Y. W. Park, A. J. Heeger, H. Shirakawa, E. J. Louis, S. C. Gau and A. G. MacDiarmid, Phys. Rev. Lett. 39, 1098 (1977).
11. C. K. Chiang, M. A. Druy, S. C. Gau, A. J. Heeger, E. J. Louis, A. G. MacDiarmid, Y. W. Park, J. Amer. Chem. Soc. 100 (1013) (1978).
12. C. K. Chiang, Y. W. Park, A. J. Heeger, H. Shirakawa, E. J. Louis, and A. G. MacDiarmid, J. Chem. Phys. (in press) (1978).
13. C. K. Chiang, S. C. Gau, C. R. Fincher, Jr., Y. W. Park, A. G. MacDiarmid, and A. J. Heeger, Appl. Phys. Lett. (in press) (1978)
14. Y. W. Park, M. A. Druy, C. K. Chiang, A. G. MacDiarmid, A. J. Heeger, H. Shirakawa, and S. Ikeda, Phys. Rev. Lett. (Submitted).
15. C. R. Fincher, Jr., D. L. Peebles, A. J. Heeger, M. A. Druy, Y. Matsumura, A. G. MacDiarmid, H. Shirakawa and S. Ikeda, Solid State Commun. (in press) (1978).
16. The successful doping and resulting control of electrical properties over a wide range, including high conductivity (in the metallic range) at heavy doping levels have now been reproduced in many laboratories throughout the world. See, for example, J. F. Kwak, T. C. Clarke, R. L. Greene, and G. B. Street, Bull. Am. Phys. Soc. 23, 56 (1978).
17. For a summary and detailed references see A. A. Ovchinnikov, Soviet Phys. Uspekhi 15, 575 (1973).

TECHNICAL REPORT DISTRIBUTION LIST, GEN

	No. Copies
Office of Naval Research Attn: Code 472 800 North Quincy Street Arlington, Virginia 22217	2
ONR Branch Office Attn: Dr. George Sandoz 536 S. Clark Street Chicago, Illinois 60605	1
ONR Branch Office Attn: Scientific Dept. 715 Broadway New York, New York 10003	1
ONR Branch Office 1030 East Green Street Pasadena, California 91106	1
ONR Branch Office Attn: Dr. L. H. Peebles Building 114, Section D 666 Summer Street Boston, Massachusetts 02210	1
Director, Naval Research Laboratory Attn: Code 6100 Washington, D.C. 20390	1
The Assistant Secretary of the Navy (R,E&S) Department of the Navy Room 4E736, Pentagon Washington, D.C. 20350	1
Commander, Naval Air Systems Command Attn: Code 310C (H. Rosenwasser) Department of the Navy Washington, D.C. 20360	1
Defense Documentation Center Building 5, Cameron Station Alexandria, Virginia 22314	12
Dr. Fred Saalfeld Chemistry Division Naval Research Laboratory Washington, D.C. 20375	1
U.S. Army Research Office Attn: CRD-AA-IP P.O. Box 1211 Research Triangle Park, N.C. 27709	1
Naval Ocean Systems Center Attn: Mr. Joe McCartney San Diego, California 92152	1
Naval Weapons Center Attn: Dr. A. B. Amster, Chemistry Division China Lake, California 93555	1
Naval Civil Engineering Laboratory Attn: Dr. R. W. Drisko Port Hueneme, California 93401	1
Department of Physics & Chemistry Naval Postgraduate School Monterey, California 93940	1
Dr. A. L. Slafkosky Scientific Advisor Commandant of the Marine Corps (Code RD-1) Washington, D.C. 20380	1
Office of Naval Research Attn: Dr. Richard S. Miller 800 N. Quincy Street Arlington, Virginia 22217	1
Naval Ship Research and Development Center Attn: Dr. G. Bosmajian, Applied Chemistry Division Annapolis, Maryland 21401	1
Naval Ocean Systems Center Attn: Dr. S. Yamamoto, Marine Sciences Division San Diego, California 91232	1
Mr. John Boyle Materials Branch Naval Ship Engineering Center Philadelphia, Pennsylvania 19112	1

TECHNICAL REPORT DISTRIBUTION LIST, 356B

	No. Copies
Dr. T. C. Williams Union Carbide Corporation Chemical and Plastics Tarrytown Technical Center Tarrytown, New York	1
Dr. R. Soulen Contract Research Department Pennwalt Corporation 900 First Avenue King of Prussia, Pennsylvania 19406	1
Dr. A. G. MacDiarmid University of Pennsylvania Department of Chemistry Philadelphia, Pennsylvania 19174	1
Dr. C. Pittman University of Alabama Department of Chemistry University, Alabama 35486	1
Dr. H. Allcock Pennsylvania State University Department of Chemistry University Park, Pennsylvania 16802	1
Dr. M. Kenney Case-Western University Department of Chemistry Cleveland, Ohio 44106	1
Dr. R. Lenz University of Massachusetts Department of Chemistry Amherst, Massachusetts 01002	1
Dr. M. David Curtis University of Michigan Department of Chemistry Ann Arbor, Michigan 48105	1
Dr. M. Good Division of Engineering Research Louisiana State University Baton Rouge, Louisiana 70803	1
Douglas Aircraft Company 3855 Lakewood Boulevard Long Beach, California 90846 Attn: Technical Library C1 290/36-84 AUTO-Sutton	1
NASA-Lewis Research Center 21000 Brookpark Road Cleveland, Ohio 44135 Attn: Dr. T. T. Serafini, MS 49-1	1
Dr. J. Griffith Naval Research Laboratory Chemistry Section, Code 6120 Washington, D.C. 20375	1
Dr. G. Goodman Globe-Union Incorporated 5757 North Green Bay Avenue Milwaukee, Wisconsin 53201	1
Dr. E. Fischer, Code 2853 Naval Ship Research and Development Center Annapolis Division Annapolis, Maryland 21402	1
Dr. Martin H. Kaufman, Head Materials Research Branch (Code 4542) Naval Weapons Center China Lake, California 93555	1
Dr. J. Magill University of Pittsburg Metallurgical and Materials Engineering Pittsburg, Pennsylvania 22230	1
Dr. C. Allen University of Vermont Department of Chemistry Burlington, Vermont 05401	1
Dr. D. Bergbreiter Texas A&M University Department of Chemistry College Station, Texas 77843	1

TECHNICAL REPORT DISTRIBUTION LIST, 356B

	No. Copies
Professor R. Drago Department of Chemistry University of Illinois Urbana, Illinois 61801	1
Dr. F. Brinkman Chemical Stability & Corrosion Division Department of Commerce National Bureau of Standards Washington, D.C. 20234	1
Professor H. A. Titus Department of Electrical Engineering Naval Postgraduate School Monterey, California 93940	1
COL B. E. Clark, Code 100M Office of Naval Research 800 N. Quincy Street Arlington, Virginia 22217	1
Professor T. Katz Department of Chemistry Columbia University New York, New York 10027	1
Dr. Frank Karasz Department of Polymer Science and Engineering University of Massachusetts Amherst, Massachusetts 01003	1
Dr. James Chien Department of Polymer Science and Engineering University of Massachusetts Amherst, Massachusetts 01003	1
Professor A. J. Heeger Director Laboratory for Research on Structure of Matter 33rd and Walnut Streets/K1 University of Pennsylvania Philadelphia, Pennsylvania 19104	1
Dr. Richard A. Reynolds Deputy Director Defense Sciences Office DARPA 1400 Wilson Blvd. Arlington, Virginia 22209	1
Dr. Rudolph J. Marcus Office of Naval Research Scientific Liaison Group American Embassy APO San Francisco 96503	1
Mr. James Kelley DTNSRDC Code 2803 Annapolis, Maryland 21402	1

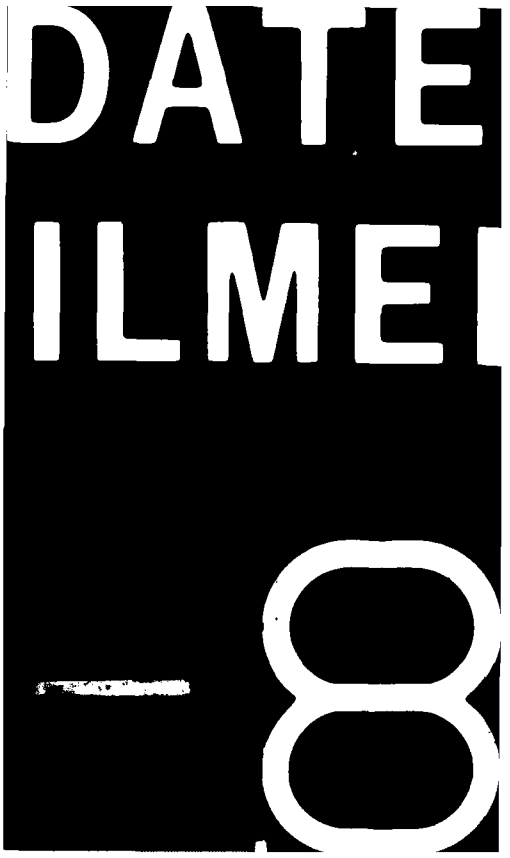
DATE
ILME
8